Biochemical and Biophysical Research Communications 377 (2008) 35–40

Contents lists available at ScienceDirect

Biochemical and Biophysical Research Communications

journal homepage: www.elsevier.com/locate/ybbrc

Quantum dots for tracking cellular transport of lectin-functionalized nanoparticles

Xiaoling Gao [a,c], Tao Wang [b], Bingxian Wu [a], Jun Chen [a], Jiyao Chen [b], Yang Yue [d], Ning Dai [d], Hongzhuan Chen [c,*], Xinguo Jiang [a,*]

[a] Department of Pharmaceutics, School of Pharmacy, Fudan University, Shanghai 200032, PR China
[b] Surface Physics Laboratory (National Key Laboratory), Physics Department, Fudan University, Shanghai 200433, PR China
[c] Department of Pharmacology, Institute of Medical Sciences, Shanghai Jiaotong University School of Medicine, Shanghai 200025, PR China
[d] National Laboratory for Infrared Physics, Shanghai Institute of Technical Physics, Chinese Academy of Sciences, Shanghai 200083, PR China

ARTICLE INFO

Article history:
Received 3 September 2008
Available online 25 September 2008

Keywords:
Quantum dots
Fluorescent probe
Nanoparticles
Transport
Caco-2 cells

ABSTRACT

Successful drug delivery by functionalized nanocarriers largely depends on their efficient intracellular transport which has not yet been fully understood. We developed a new tracking technique by encapsulating quantum dots into the core of wheat germ agglutinin-conjugated nanoparticles (WGA-NP) to track cellular transport of functionalized nanocarriers. The resulting nanoparticles showed no changes in particle size, zeta potential or biobinding activity, and the loaded probe presented excellent photostability and tracking ability. Taking advantage of these properties, cellular transport profiles of WGA-NP in Caco-2 cells was demonstrated. The cellular uptake begins with binding of WGA to its receptor at the cell surface. The subsequent endocytosis happened in a cytoskeleton-dependent manner and by means of clathrin and caveolae-mediated mechanisms. After endosome creating, transport occurs to both trans-Golgi and lysosome. Our study provides new evidences for quantum dots as a cellular tracking probe of nanocarriers and helps understand intracellular transport profile of lectin-functionalized nanoparticles.

Development of nanocarriers (e.g., liposomes, micelles, polymeric nanoparticles, and dendrimers) has provided a promising approach to obtain desirable biopharmaceutic and pharmacokinetic properties for medicines and become one of the most important areas of nanomedicine. A particular interest is focused on the development of functionalized nanocarriers obtained by attaching ligands such as antibodies, glycoproteins, peptides and carbohydrates to the surface of nanocarrier for selective delivery of medicines to target areas in the body. Lectins, proteins or glycoproteins of nonimmunological origin, recognizing sugar molecule specifically and therefore capable of binding glycosylated membrane components, have been widely developed to conjugate with nanocarriers for efficient drug delivery [1–3]. For example, wheat germ agglutinin (WGA) from Triticum vulgare, specifically binding to *N*-acetyl-D-glucosamine and sialic acid which is abundantly observed in both intestine [3] and nasal cavity [4], has now been exploited in lectin-functionalized nanoparticles for improved bioavailability and site-specific drug delivery in our laboratory and others [2,3,5,6]. It is highly suggested that successful delivery of drugs by the functionalized nanocarriers largely depends on their safe and efficient cellular transport. Therefore, it is of great importance to develop novel approaches for elucidation of the intracellular transport profiles of lectin-functionalized nanoparticles upon their extensive application.

Quantum dots (QDs) are fluorescent semiconductor nanocrystals characterized by unique physical, chemical and optical properties and are now emerging as a revolutionary means for imaging and optical detection [7,8]. Compared with organic dyes, QDs exhibit high extinction coefficients, much reduced photobleaching rates and narrow size-tunable emission spectra [7,8]. Application of QDs in pharmaceutics for tracking nanocarriers (e.g. liposomes, micelles, polymeric nanoparticles, and dendrimers) might shed new light on understanding the interaction between drug delivery systems and biological system. The purpose of this study is to address the feasibility of QDs to serve as fluorescent probes for drug delivery systems and to study the intracellular transport profiles of WGA-functionalized poly (ethylene glycol)-poly (lactic acid) (PEG-PLA) nanoparticles (WGA-NP). To achieve this goal, high-quality, hydrophobic QDs — tri-*n*-octylphosphine oxide-coated CdSe/ZnS QDs (TOPO-QDs) were encapsulated into PEG-PLA nanoparticles which were then functionalized with WGA to their surface. Particle size, zeta potential, photostability of the resulting nanoparticles and tracking ability of the loaded QDs were evaluated to address the feasibility of the probing technique. Caco-2 cells, human colon

* Corresponding authors. Fax: +86 21 54237381.
E-mail addresses: yaoli@shsmu.edu.cn (H. Chen), xgjiang@shmu.edu.cn (X. Jiang).

0006-291X/$ - see front matter © 2008 Elsevier Inc. All rights reserved.
doi:10.1016/j.bbrc.2008.09.077

carcinoma cells with WGA-binding sugars extensively expressed on the cell surface [2,9], were used as a cell model to study the cellular transport profiles of WGA-NP.

Materials and methods

Materials. Methyl-PEG-PLA and maleimide-PEG-PLA were synthesized by means of ring opening polymerization [5]. TOPO-QDs were prepared at elevated temperatures in TOPO as described previously [10]. WGA was obtained from Vector Laboratories; 2-iminothiolane hydrochloride (2-IT), from Sigma; 5,5-dithiobis (2-nitrobenzoic acid) (Ellman's reagent), from Acros (Belgium); Dulbecco's Modified Eagle Medium (DMEM) (high glucose) and fetal bovine serum (FBS) from Gibco (Invitrogen, USA). Both LysoTracker Green and BODIPY-Cer complexed to BSA were purchased from Molecular Probe, Invitrogen (USA). NaN_3 was kindly provided by Department of Medicinal Chemistry, School of Phamacy, Fudan University, and chlorpromazine by Shanghai Mental Health Center. Filipin was purchased from Fluka (Germany), monensin, nocodazole, cytochalasin D and Brefeldin A from *Penicillium brefeldianum* (BFA) from Sigma (USA).

Preparation and Characterization of WGA-conjugated QDs-loaded PEG-PLA nanoparticles (WGA-QDs-NP). QDs-loaded PEG-PLA nanoparticles (QDs-NP) were prepared with a blend of maleimide-PEG-PLA and methyl-PEG-PLA using an emulsion/solvent evaporation technique. Briefly, 9 mg maleimide-PEG-PLA and 1 mg methyl-PEG-PLA were dissolved in 0.5 ml of dichloromethane containing 2×10^{-6} mol/L of QDs. The solution was then emulsified by sonication (220 w, 30 s) on ice in a 2 ml of 1% aqueous sodium cholate solution. The emulsion obtained was diluted into 8 ml of a 0.5% aqueous sodium cholate solution under moderate magnetic stirring. Five minutes later, dichloromethane was evaporated at low pressure at 30 °C using Büchi rotavapor R-200 (Büchi, Germany). Then the nanoparticles were centrifuged at 21,000*g* for 45 min using TJ-25 centrifuge (Beckman Counter, USA.) equipped with an A-14 rotor. Supernatant discarded, and the obtained nanoparticles were resuspended with distilled water and subjected to a 1.5×20 cm sepharose CL-4B column to remove the unentrapped QDs. For preparing coumarin-6-loaded nanoparticles, 2×10^{-6} mol/L of coumarin-6 were dissolved in dichloromethane instead of QDs. The resulting probe-loaded nanoparticles were modified with WGA and purified as described previously [5,6].

Mean diameter and zeta potential of the resulting nanoparticles was determined by dynamic light scattering (DLS) analysis using Zeta Potential/Particle Sizer NICOMPTM 380 ZLS (Santa Barbara, California, USA.) with He–Ne lamp at 632.8 nm, respectively. For determining the internal structure of WGA-QDs-NP, nanoparticles were diluted to appropriate concentration and observed under a freeze-fracture electron microscope (JEOL 2010, JEOL, Japan).

To evaluate photostability of the novel fluorescent probe, photobleaching profiles of WGA-QDs-NP were determined under coherent laser scan (Ar ion laser, 488 nm) and compared with those of an organic dye — coumarin-6-loaded nanoparticles (WGA-coumarin-6-NP).

Tracking ability of QDs encapsulated in WGA-NP. Haemagglutination test was performed to determine whether QDs was an appropriate probe to their carriers. QDs-loaded nanoparticles and WGA-QDs-NP were incubated with 20% (v/v) suspension of fresh rat blood in 0.9% NaCl at 37 °C for 30 min and 24 h, respectively. After that, the mixtures were observed under a fluorescence microscope (Olympus IX71) and images were taken and colored with Image-Pro Plus.

Live cell imaging and intracellular distribution. Caco-2 cells were obtained from American Type Culture Collection (Rochville, MD, USA) and grown in a 5% CO_2 humidified atmosphere at 37 °C in DMEM medium supplemented with 10% FBS, 1% non-essential amino acids, 100 units/ml penicillin, and 100 μg/ml streptomycin. For live cell imaging, Caco-2 cells were plated onto multiple glass-bottom tissue culture plates (MatTek, Ashland, MA) at an initial confluency of 10–20%. Forty hours later, the cells was examined under a confocal microscope (Zeiss LSM 510) equipped with a temperature controller. WGA-QDs-NP (200 μg/ml nanoparticles, containing 20 pM QDs) were added and photos were taken one frame per minute for 2 h. After that, *Z* direction scan on the cells was performed to check if WGA-QDs-NP really entered the cells.

For intracellular distribution analysis, after 2-h incubation with WGA-QDs-NP, Caco-2 cells were washed with fresh culture medium and incubated with 50 nM LysoTracker Green (Molecular Probe, Invitrogen, USA) or 9 μg/ml BODIPY-Cer complexed to BSA (Molecular Probe, Invitrogen, USA) in FBS-free DMEM for 30 min and examined under the confocal microscope described above.

Intracellular transport profiles. To determine intracellular transport profile of WGA-QDs-NP, cellular uptake of WGA-QDs-NP was determined quantitatively with High Content Cell Analysis System. Caco-2 cells (5000 cells per well) were seeded in a 96-well Corning® cell culture plate. Thirty-six hours later, 200 μg/ml WGA-QDs-NP was added and incubated with the cells at 37 °C for 2 h. After that, the cells were washed with D-hanks buffer and fixed with 3.7% formaldehyde solution for 10 min. Stained with 2 μg/ml Hochest 33258 at room temperature, away from light for 1 h, the cell culture plate was finally washed for three times and detected under the KineticScan® HCS Reader (version 3.1, Cellomics Inc., Pittsburgh, PA, USA). Fluorescent images were captured in the two channels relevant to Hoescht and TRITC (for the quantification of QDs-loaded nanoparticles) and analyzed automatively to quantify cell number and level of intracellular WGA-QDs-NP, respectively. Analysis algorithms were obtained from Cellomics Inc. (Pittsburgh, PA, USA) and referred to as Target Activation. Three thousand cells were detected for each well ($n = 3$).

Specific nature of cellular uptake of WGA-QDs-NP was determined by inhibition experiment with specific sugar. WGA-QDs-NP (0.5 mg) was preincubated with excess chitin (0.5 mg) at 37 °C for 3 h in 0.01 M HEPES buffer (pH 8.5) containing 0.1 mM $CaCl_2$. After that, the mixtures (containing 200 μg/ml WGA-QDs-NP) were incubated with Caco-2 cells and the levels of intracellular WGA-QDs-NP were determined. Cellular endocytosis mechanism of WGA-QDs-NP was studied by preincubating the cells with 10 μg/ml of chlorpromazine for 30 min to inhibit clathrin-mediated endocytosis pathway [11], and 5 μg/ml of filipin to inhibit the caveolae-mediated one [11] before the addition of 200 μg/ml WGA-QDs-NP. Golgi apparatus destroyer — BFA (5 μg/ml) [12] and lysosome inhibitor — monensin (100 nM) [13] were used to examine the contribution of Golgi apparatus and lysosome to the cellular uptake of WGA-QDs-NP, respectively. Nocodazole (33 μM), a microtubules depolymerization agent [14] and cytochalasin D (12.5 μg/ml), a fungal metabolite that disrupts actin polymerization [14] were used to determine whether microtubules and actin filaments are involved in the cellular transport of WGA-QDs-NP. Differences between the inhibition groups and the WGA-QDs-NP (control) group were evaluated by two-sided unpaired Student's *t*-test. Differences were considered statistically significant at $P < 0.05$.

Intracellular distribution of WGA-QDs-NP was also determined in the presence of endocytosis inhibitors. Caco-2 cells were incubated for 30 min with chlorpromazine (10 μg/ml), filipin (5 μg/ml), nocodazole (33 μM), and cytochalasin D (12.5 μg/ml), respectively, before the addition of WGA-QDs-NP and incubation at 37 °C for 2 h. After that, the cells were stained with LysoTracker Green or BODIPY-Cer complexed to BSA and examined under a confocal microscope as described above.

Results and discussion

Preparation and characterization of WGA-QDs-NP

WGA-QDs-NP was prepared by encapsulating TOPO-QDs into PEG-PLA nanoparticles by an emulsion/solvent evaporation technique and then functionalizing WGA to the particle surface. The resulting nanoparticles exhibited a spherical shape with a number-based average diameter (95.3 ± 41.0 nm) comparable with that of QDs-free WGA-NP (92.0 ± 33.7 nm). Zeta potential of WGA-QDs-NP was −22.67 ± 1.21 mV, which was also similar with that of QDs-free WGA-NP (−18.9 ± 2.4 mV). Internal structure of WGA-QDs-NP demonstrated by freeze-fracture electron microscopy suggested that numerous QDs were encapsulated in each nanoparticle and most of them located at the center of the particles (Fig. 1A).

These results clearly suggested that QDs was encapsulated into the core of the PEG-PLA nanoparticles with a high payload and with no changes in the size and zeta potential of the carrier. We believed this phenomenon was mainly accounted for by the strong hydrophobic interaction between TOPO and PLA fragment of the polymer which composed the core of the resulting PEG-PLA nanoparticles [15]. In the course of primary emulsification, TOPO-QDs coating with PLA remained inside the oil droplets while the hydrophilic group — PEG migrated to the water surface. Upon solvent evaporation, the nanoparticles core solidified, forming solid nanoparticles with high stability.

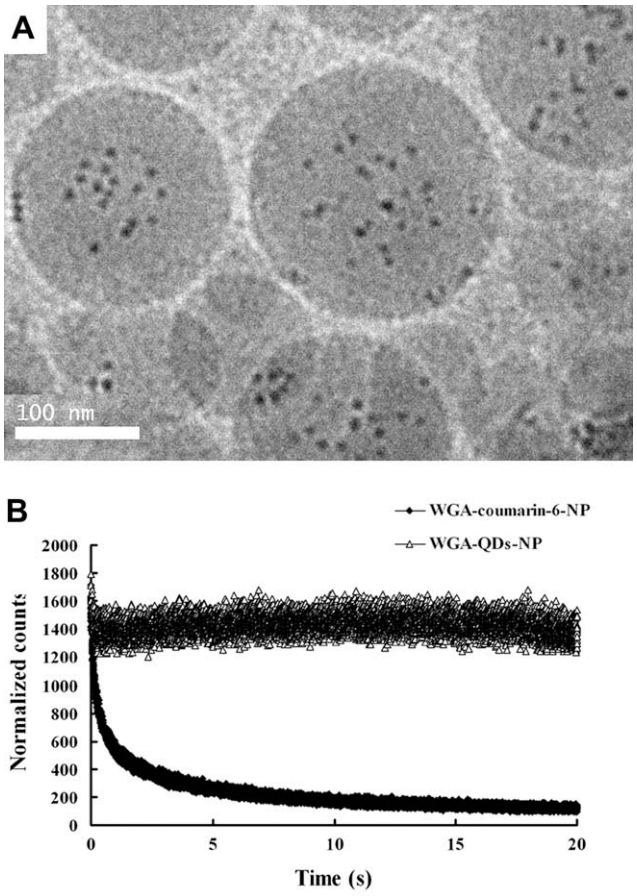

Fig. 1. (A) Internal structure of WGA-conjugated quantum dots-loaded nanoparticles (WGA-QDs-NP) exhibited by freeze-fracture electron microscopy. Bar, 100 nm. (B) Photobleaching profiles of WGA-QDs-NP and WGA-conjugated coumarin-6-loaded PEG-PLA nanoparticles (WGA-coumarin-6-NP) under a continuously-irradiating Ar ion laser (488 nm), respectively.

Optical properties of WGA-QDs-NP were determined and compared with those of an organic dye — coumarin-6-loaded nanoparticles at the same molar level and similar fluorescent intensity. Fluorescence of WGA-coumarin-6-NP bleached quickly under a coherent 488 nm Ar ion laser scan with a half quench time less than 0.5 s while that of WGA-QDs-NP remained constant for more than 20 s (Fig. 1B), which strongly indicated that QDs presented much better photostability compared with organic dyes and may be attractive probes particularly for long-term staining and quantitative evaluation.

Tracking ability of QDs encapsulated in WGA-NP

To determine the tracking ability of QDs, observation on the QDs-loaded nanoparticles was made under a fluorescent microscope after their incubation with erythrocytes. After incubation with WGA-QDs-NP, erythrocytes were agglutinated due to the haemagglutination effect of WGA and almost all the red fluorescence of QDs remained stuck to the cells even after more than 24 h incubation (Supplementary data Fig. 1C and D). But in the case of the unmodified QDs-loaded nanoparticles, the red fluorescence of QDs dispersed at random and didn't show any specific affinity to erythrocytes (Supplementary data Fig. 1A and B). The difference clearly suggested that the incorporation of QDs did not change the bioactivity of the surface-conjugated lectin and the loaded probe can track their carriers properly for a long time. Compared with those fluorescent probes such as carboxyfluorescein [16] and nile red [17] which are prone to leak from their carriers after contact with cells, QDs can be a far more stable fluorescent probe. It was supposed that this was mainly benefited from the bigger size and higher hydrophobicity of TOPO-QDs over the organic dyes.

Live cell imaging and intracellular distribution

Uptake of WGA-QDs-NP in live Caco-2 cells was examined under a confocal microscope equipped with a temperature controller. Following the addition of WGA-QDs-NP, time-dependent accumulation of the functionalized nanoparticle to the surface of the cell pellet and rapid uptake (<10 min) into the cells were observed (Fig. 2A). Effective delivery of WGA-NP into Caco-2 cells was confirmed by *Z* scan (Fig. 2B). To determine the intracellular distribution of WGA-QDs-NP, Golgi apparatus and lysosome were labeled with BODIPY-Cer complexed to BSA and LysoTracker Green, respectively. Colocalization of the functionalized nanoparticles with both Golgi apparatus (Fig. 2C) and lysosome (Fig. 2D) were observed, suggesting that WGA-NP could be transported to both of these organelles.

These findings not only provide new insights into the cellular transport of WGA-NP but also provide new evidences for quantum dots as a cellular tracking probe of nanocarriers. Fluorescent labels such as FITC, rhodamine, and coumarin have been used as probes to study the binding, internalization, and cellular transport of nanoparticles. However, due to their limitation in photostability for extended imaging, limited spatial and temporal resolution, these probes allows for only a coarse observation on the processes which are expected to be very dynamic. The recent development of QDs for live cell imaging provides novel tools for investigating dynamic cellular transport of nanoparticles [18,19]. However, the sizes for these QDs-based nanoparticles were less than 40 nm [18,19], much smaller than those of most nanocarriers intended for drug delivery. Since the size of nanoparticles greatly influences their cellular fates [20], it is hard to predict that the larger particles would undergo the same cellular transport profiles as the smaller ones. In this contribution, particle size of the functionalized nanoparticles remained unchanged after their loading with QDs. Therefore, the advantage of this method would be obvious for real-time

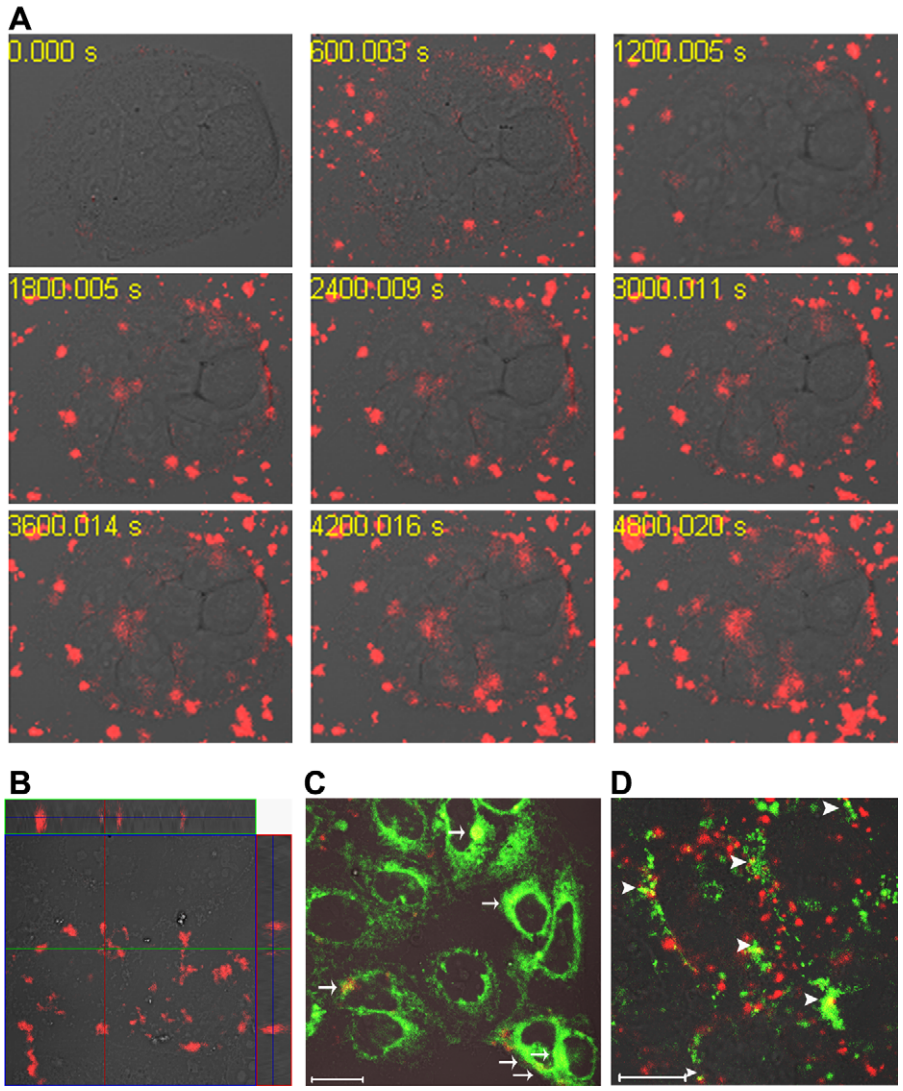

Fig. 2. Cellular uptake and intracellular distribution of WGA-QDs-NP in Caco-2 cells. (A) Dynamic process of cellular accumulation and uptake of WGA-QDs-NP in live Caco-2 cells. Photos taken one frame per minute for 2 h after the addition of WGA-QDs-NP. (B) Entry of WGA-QDs-NP into the cells showed by *Z* scan. (C) Colocalization (yellow, indicated with arrow) of WGA-QDs-NP (red) and Golgi apparatus (green). (D) Colocalization (yellow, indicated with arrow head) of WGA-QDs-NP (red) and lysosome (green). Bar, 20 μm. (For interpretation of color mentioned in this figure the reader is referred to the web version of the article.)

tracking of cellular endocytosis, exocytosis and intracellular transport of functionalized nanocarriers.

Intracellular transport profiles

Inhibition experiments were performed to elucidate the transport mechanism. High Content Cell Analysis System, an automated platform for performing fluorescence microscopy and quantitative image analysis was used to quantify cellular uptake of WGA-QDs-NP. Specific nature of cellular uptake of WGA-QDs-NP was determined by inhibition experiment with specific sugar — chitin. It was found that preincubation with excess chitin significantly reduced cellular uptake of WGA-QDs-NP (Fig. 3A), suggesting that interactions between Caco-2 cells and WGA-QDs-NP were mainly due to the immobilization of carbohydrate-binding pockets on the surface of nanoparticles. Endocytosis pathway of WGA-QDs-NP was determined by adding pharmacological inhibitors of clathrin-mediated endocytosis — chlorpromazine and inhibitors of caveolae-mediated endocytosis — filipin into the mediums, respectively. Both of them reduced the cellular uptake of WGA-QDs-NP (Fig. 3A), suggesting that WGA-QDs-NP was absorbed via both clathrin and caveolae-dependent endocytosis pathways. Both BFA and monensin reduced the uptake of WGA-QDs-NP (Fig. 3A), once again confirming the involvement of both Golgi apparatus and lysosome in intracellular transport of WGA-QDs-NP. Both nocodazole and cytochalasin D significantly reduced cellular uptake of WGA-QDs-NP, implying that the transport is both microtubules and actin filaments dependent (Fig. 3A).

Intracellular distribution of WGA-QDs-NP was also determined at the presence of endocytosis inhibitors. Inhibitions of both clathrin and caveolae-mediated pathways greatly suppressed cellular delivery of WGA-QDs-NP, which also reduced the colocation of WGA-QDs-NP and lysosome and Golgi apparatus (Fig. 3B and C), once again confirming the involvement of these two pathways in cellular internalization and distribution. In the case of inhibiting cytoskeleton using nocodazole and cytochalasin D, colocation of WGA-QDs-NP and lysosome reduced (Fig. 3C), indicating that cellular transport of WGA-QDs-NP to lysosome is dependent on both microtubules and actin filaments. In contrast, accumulation of WGA-QDs-NP in Golgi apparatus did not reduce but increased at

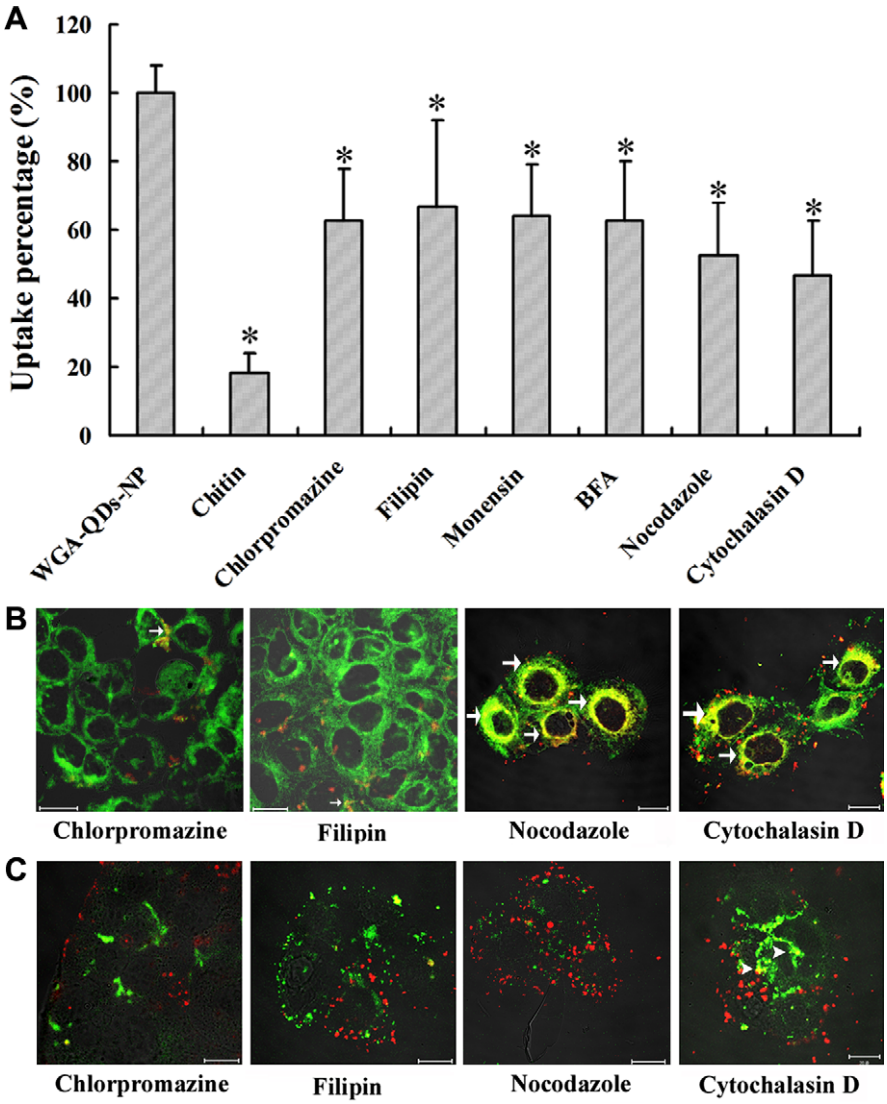

Fig. 3. (A) Cellular uptake of WGA-QDs-NP at the presence of various inhibitors determined quantitatively with High Content Cell Analysis System. Chitin: WGA-QDs-NP preincubated with excess chitin at 37 °C for 3 h before their incubation with Caco-2 cells at 37 °C for 2 h. Chlorpromazine (10 μg/ml), filipin (5 μg/ml), BFA (5 μg/ml), monensin (100 nM), nocodazole (33 μM) and cytochalasin D (12.5 μg/ml) preincubated with Caco-2 cells at 37 °C for 30 min before the addition of WGA-QDs-NP and incubation at 37 °C for 2 h, respectively. *Significantly different from the cellular uptake of WGA-QDs-NP at the absence of inhibitors. (B) Colocalization of WGA-QDs-NP and Golgi apparatus (yellow, indicated with arrow) in Caco-2 cells at the presence of chlorpromazine, filipin, nocodazole and cytochalasin D, respectively. (C) Colocalization of WGA-QDs-NP and lysosome (yellow, indicated with arrow head) in Caco-2 cells at the presence of chlorpromazine, filipin, nocodazole and cytochalasin D, respectively. Bar, 20 μm. (For interpretation of color mentioned in this figure the reader is referred to the web version of the article.)

the presence of both nocodazole and cytochalasin D (Fig. 3B). Since it has been well documented that both microtubules and actin filaments play a key role in efficient post-Golgi trafficking [21], we believed that the accumulation of WGA-QDs-NP in Golgi apparatus following cytoskeleton inhibition was mainly resulted from the blocking of post-Golgi trafficking.

Consistent with cellular transport profiles of WGA [22,23], endocytosis of WGA-NP begins with binding of WGA to N-acetylglucosamine or sialic acid on the cell surface and includes both clathrin and caveolae-mediated mechanisms. After endosome creating, transport occurs to both trans-Golgi and lysosomes. Cytoskeleton including microtubule and actin filaments was involved in cellular trafficking of WGA-NP. Such elucidation of cellular trafficking pathway of WGA-NP may help in rational design of novel drug delivery systems. For example, Lysosome participation in intracellular transport of WGA-NP indicates that replacement of PEG-PLA with polymers (eg. PEG-PLGA) with better lysosome escape ability may improve the stability of certain loaded agents.

All in all, in this paper, we firstly reported the application of lipophilic QDs — TOPO-coated QDs as sensitive and stable fluorescent probes for a nano-delivery system — WGA-functionalized PEG-PLA nanoparticles. By taking advantages of the excellent photostability and tracing ability of QDs, cellular transport profile of WGA-NP in Caco-2 cells was demonstrated. The technique described here clearly indicated that QDs might serve as an excellent fluorescent probe for both qualitative and quantitative tracking of nanocarriers in the biological systems.

Acknowledgments

The study was supported by National Key Basic Research Program (2007CB935800), National Natural Science Foundation of China (No. 30801442), and Grants from Shanghai Education Committee and Institute of Medical Sciences, Shanghai Jiaotong University School of Medicine.

Appendix A. Supplementary data

Supplementary data associated with this article can be found, in the online version, at doi:10.1016/j.bbrc.2008.09.077.

References

[1] C.M. Lehr, Lectin-mediated drug delivery: the second generation of bioadhesives, J. Control Release 65 (2000) 19–29.
[2] G.J. Russell-Jones, H. Veitch, L. Arthur, Lectin-mediated transport of nanoparticles across Caco-2 and OK cells, Int. J. Pharm. 190 (1999) 165–174.
[3] F. Gabor, E. Bogner, A. Weissenboeck, M. Wirth, The lectin–cell interaction and its implications to intestinal lectin-mediated drug delivery, Adv. Drug Deliv. Rev. 56 (2004) 459–480.
[4] G. Berger, T. Kogan, E. Skutelsky, D. Ophir, Glycoconjugate expression in normal human inferior turbinate mucosa: a lectin histochemical study, Am. J. Rhinol. 19 (2005) 97–103.
[5] X. Gao, W. Tao, W. Lu, Q. Zhang, Y. Zhang, X. Jiang, S. Fu, Lectin-conjugated PEG-PLA nanoparticles: preparation and brain delivery after intranasal administration, Biomaterials 27 (2006) 3482–3490.
[6] X. Gao, B. Wu, Q. Zhang, J. Chen, J. Zhu, W. Zhang, Z. Rong, H. Chen, X. Jiang, Brain delivery of vasoactive intestinal peptide enhanced with the nanoparticles conjugated with wheat germ agglutinin following intranasal administration, J. Control Release 121 (2007) 156–167.
[7] W.C. Chan, D.J. Maxwell, X. Gao, R.E. Bailey, M. Han, S. Nie, Luminescent quantum dots for multiplexed biological detection and imaging, Curr. Opin. Biotechnol. 13 (2002) 40–46.
[8] M. Bruchez Jr., M. Moronne, P. Gin, S. Weiss, A.P. Alivisatos, Semiconductor nanocrystals as fluorescent biological labels, Science 281 (1998) 2013–2016.
[9] F. Gabor, M. Stangl, M. Wirth, Lectin-mediated bioadhesion: binding characteristics of plant lectins on the enterocyte-like cell lines Caco-2, HT-29 and HCT-8, J. Control Release 55 (1998) 131–142.
[10] W.W. Yu, L. Qu, W. Guo, X. Peng, Experimental determination of the extinction coefficient of CdTe, CdSe, and CdS nanocrystals, Chem. Mater. 15 (2003) 2854–2860.
[11] Y. Mo, L.Y. Lim, Mechanistic study of the uptake of wheat germ agglutinin-conjugated PLGA nanoparticles by A549 cells, J. Pharm. Sci. 93 (2004) 20–28.
[12] S. Jiang, S.W. Rhee, P.A. Gleeson, B. Storrie, Capacity of the Golgi apparatus for cargo transport prior to complete assembly, Mol. Biol. Cell 17 (2006) 4105–4117.
[13] F. Gabor, A. Schwarzbauer, M. Wirth, Lectin-mediated drug delivery: binding and uptake of BSA-WGA conjugates using the Caco-2 model, Int. J. Pharm. 237 (2002) 227–239.
[14] M.M. Zegers, K.J. Zaal, S.C. van IJzendoorn, K. Klappe, D. Hoekstra, Actin filaments and microtubules are involved in different membrane traffic pathways that transport sphingolipids to the apical surface of polarized HepG2 cells, Mol. Biol. Cell 9 (1998) 1939–1949.
[15] R. Gref, Y. Minamitake, M.T. Peracchia, V. Trubetskoy, V. Torchilin, R. Langer, Biodegradable long-circulating polymeric nanospheres, Science 263 (1994) 1600–1603.
[16] J. Van Renswoude, D. Hoekstra, Cell-induced leakage of liposome contents, Biochemistry 20 (1981) 540–546.
[17] P. Pietzonka, B. Rothen-Rutishauser, P. Langguth, H. Wunderli-Allenspach, E. Walter, H.P. Merkle, Transfer of lipophilic markers from PLGA and polystyrene nanoparticles to caco-2 monolayers mimics particle uptake, Pharm. Res. 19 (2002) 595–601.
[18] G. Ruan, A. Agrawal, A.I. Marcus, S. Nie, Imaging and tracking of tat peptide-conjugated quantum dots in living cells new insights into nanoparticle uptake, intracellular transport, and vesicle shedding, J. Am. Chem. Soc. 129 (2007) 14759–14766.
[19] A. Cambi, D.S. Lidke, D.J. Arndt-Jovin, C.G. Figdor, T.M. Jovin, Ligand-conjugated quantum dots monitor antigen uptake and processing by dendritic cells, Nano Lett. 7 (2007) 970–977.
[20] J. Rejman, V. Oberle, I.S. Zuhorn, D. Hoekstra, Size-dependent internalization of particles via the pathways of clathrin- and caveolae-mediated endocytosis, Biochem. J. 377 (2004) 159–169.
[21] F. Lázaro-Diéguez, C. Colonna, M. Cortegano, M. Calvo, S.E. Martínez, G. Egea, Variable actin dynamics requirement for the exit of different cargo from the trans-Golgi network, FEBS Lett. 581 (2007) 3875–3881.
[22] T.J. Raub, M.J. Koroly, R.M. Roberts, Endocytosis of wheat germ agglutinin binding sites from the cell surface into a tubular endosomal network, J. Cell Physiol. 143 (1990) 1–12.
[23] B. Peruzzo, F.E. Pastor, J.L. Blázque, P. Amat, E.M. Rodríguez, Polarized endocytosis and transcytosis in the hypothalamic tanycytes of the rat, Cell Tissue Res. 317 (2004) 147–164.